JGR Oceans

RESEARCH ARTICLE
10.1029/2018JC014707

Special Section:
Recent Progresses in Oceanography and Air-Sea Interactions in Southeast Asian Archipelago

The Fate of Surface Freshwater Entering the Indonesian Seas

Shinichiro Kida[1], Kelvin J. Richards[2], and Hideharu Sasaki[3]

[1]Research Institute for Applied Mechanics, Kyushu University, Kasuga, Japan, [2]Department of Oceanography, University of Hawai'i at Mānoa, Honolulu, HI, USA, [3]Application Laboratory, Japan Agency for Marine-Earth Science and Technology, Yokohama, Japan

Abstract The Indonesian Seas receive one of the largest amounts of rainfall around the globe. Part of this freshwater disperses to the Indian Ocean through the Indonesian Throughflow (ITF), the Pacific and Indian interocean exchange flow, making the Indonesian Seas a major source of freshwater, and plays an important part of the global hydrological cycle. By using a Lagrangian particle tracking model, we examine the pathways behind the dispersion of freshwater that the Indonesian Seas receive through precipitation. The model suggests that the dispersion from the near-surface water of the Indonesian Seas occurs in about 6 months, primarily through advection to the surrounding seas, followed by evaporation, entrainment, and vertical mixing. The Lombok Strait and the Timor Strait are the major outflowing straits, and the freshwater exiting through these straits are found to originate from limited areas and seasons. The sources for the Lombok Strait outflow are the Java Sea precipitated freshwater during boreal fall and winter, while the sources for the Timor Strait outflow are the Flores-Banda Seas and Arafura Sea precipitated freshwater during winter and spring. Mixing with the thermocline water is found to occur when the monsoonal winds induce upwelling events in winter and summer, along the shelf breaks and steep coastlines surrounding the Flores-Banda Seas. Vertical mixing provides a pathway for the surface freshwater to enter the ITF thermocline, and our model suggests that it is the Java Sea precipitated freshwater during winter that is entering the ITF thermocline along its main pathway.

Key Points:
- The fate of precipitated origin freshwater of the Indonesian Seas is examined using a Lagrangian particle tracking model
- Freshwater outflows from the Indonesian Seas to the Indian Ocean near the surface occur mostly through the Lombok and Timor Straits
- Vertical mixing to the Indonesian Throughflow thermocline water occurs along shelf breaks and coastlines during the upwelling seasons

Supporting Information:
- Supporting Information S1

Correspondence to:
S. Kida,
kida@riam.kyushu-u.ac.jp

Citation:
Kida, S., Richards, K. J., & Sasaki, H. (2019). The fate of surface freshwater entering the Indonesian Seas. *Journal of Geophysical Research: Oceans*, *124*, 3228–3245. https://doi.org/10.1029/2018JC014707

Received 23 OCT 2018
Accepted 15 APR 2019
Accepted article online 22 APR 2019
Published online 22 MAY 2019

©2019. American Geophysical Union. All Rights Reserved.

1. The Hydrological Cycle of the Indonesian Seas

The Indonesian Seas lie underneath a region of active atmospheric convection, an important component of the global hydrological cycle (Neale & Slingo, 2003; Yamanaka et al., 2018). These seas receive one of the largest amounts of the annual rainfall around the globe and thus serve as a major gateway for freshwater input to the ocean (Figure 1). Observations from Tropical Rainfall Measuring Mission (Huffman et al., 2010) show annual rainfall of roughly 170 mSv (mSv=1×10^3 m^3/s) directly to the Indonesian Seas, which is as large as the annual discharge rate of the Amazon River (Dai & Trenberth, 2002). With the global hydrological cycle anticipated to change in the presence of climate change (Held & Soden, 2006), the hydrological cycle of the Indonesian Seas will also likely change. This can affect the Indonesian Throughflow (ITF), the Pacific and Indian interocean exchange flow, and lead to changes in the salinity and, possibly, the sea level of the Indian Ocean (Llovel & Lee, 2015). However, how the freshwater that enters the Indonesian Seas disperses to the surrounding seas remains unknown. While our understandings of the transports through the various straits of the Indonesian Seas have significantly advanced during the past decade or so (see Sprintall et al., 2009, and reference therein), we have yet to understand the hydrological cycle.

Precipitation over the Indonesian Seas is modulated by the monsoons (Figures 2e–2h). Maximum monthly precipitation is observed from January to February (~240 mSv), during the northwestern monsoon. Precipitation becomes weaker around April and October, during the transition period, and a minimum is observed around August (~120 mSv), during the southeastern monsoon. Part of the precipitated water over land enters the Indonesian Seas through rivers but its sum appears to be about 10 mSv (Meybeck & Ragu, 1995; van Beek et al., 2013), which is an order less compared to that entering directly through the ocean surface.

The direct impact of precipitation on the ocean is to reduce the sea surface salinity (SSS). Studies on the SSS in the Indonesian Seas (Figures 2a–2d) show the importance of local surface fluxes as well as oceanic

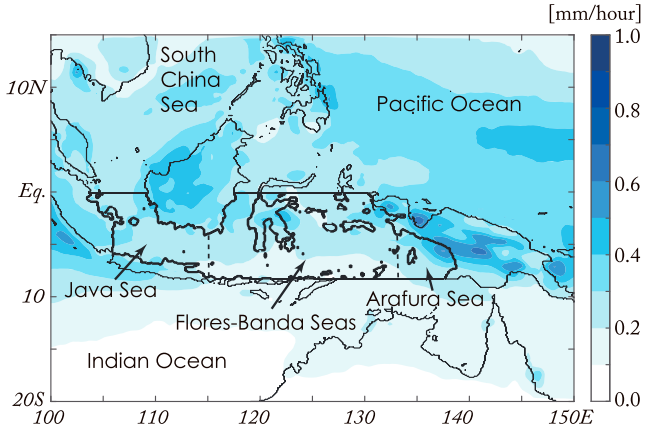

Figure 1. The climatological annual mean rainfall rate based on Tropical Rainfall Measuring Mission from 1998 to 2016. The areas surrounded by the thick solid line is how we define as the Indonesian Seas. The dashed lines along 115°E and 133°E are where we define as the boundaries of the three regions: The Java Sea (105–115°E), the Flores-Banda Seas (115–133°E), and the Arafura Sea (133–140°E).

processes (Halkides et al., 2011; Miyama et al., 1996). The Java Sea shows the lowest SSS throughout the year because of its strong rainfall and shallow bathymetry, making this region a source of freshwater (Gordon, 2005; Wyrtki, 1961). This sea is also considered a major pathway of freshwater from the South China Sea (SCS) to the Indian Ocean on an annual average (Fang et al., 2009). The seasonal cycle of the SSS in the Java Sea shows a strong semiannual signal, which is created by the monsoonal wind-driven flow and the movement of the SSS minimum. The northwest monsoonal wind-driven flow advects the fresh Java Sea water toward the Flores-Banda Seas, while the southwest monsoonal wind-driven flow advects the fresh Java Sea water toward the SCS. Recent satellite observations show the fresh Java Sea water also advected to the Indian Ocean through the Sunda Strait (Potemra et al., 2016; Susanto et al., 2016) although its magnitude and annual cycle is still unclear. The SSS of the Flores-Banda Seas and the Arafura Sea, on the other hand, show an annual cycle that is primarily controlled by the oceanic flow field (Halkides et al., 2011; Miyama et al., 1996). Low (High) SSS is observed in the Flores-Banda Seas when the fresh Java Sea origin water enters (exits) the region during the northwestern (southeastern) monsoon. High SSS is observed in the Arafura Sea when the southeast monsoonal wind induces upwelling and brings higher salinity subsurface water to the surface (Halkides et al., 2011). This seasonal upwelling event, occurring near the shelf break between the Arafura Sea and the Banda Sea, is also known to cool the sea surface temperature (Gordon & Susanto, 2001; Kida & Richards, 2009).

The Indonesian Seas have a unique role in the global ocean circulation as the gateway of the water mass exchange between the Pacific Ocean and the Indian Ocean near the equator, known as the ITF. In terms of transport, the main route is observed through the Makassar Strait, and the eastern route through the Halmahera Sea and its surrounding seas is considered secondary. The fresh surface water of the Indonesian Seas can affect this ITF, while it flows through the Indonesian Seas (Gordon, 2005; Figures 3a and 3b). The Indonesian Seas are also considered a region of strong tidal mixing (Ffield & Gordon, 1996; Nagai & Hibiya, 2015). Observations show the ITF is characterized by high salinity thermocline water of the North Pacific when it enters from the Makassar Strait but exit as fresh thermocline water as a result of mixing between fresh surface and fresh intermediate water (Ffield & Gordon, 1996; Koch-Larrouy et al., 2008). The ITF water thus becomes a source of freshwater for the Indian Ocean (Gordon, 2005; Koch-Larrouy et al., 2008; Wyrtki, 1961).

What is the fate of the freshwater that enters the Indonesian Seas? The freshwater should either evaporate back to the atmosphere, be advected, or enter the ITF thermocline water. The observed 50-year trend in salinity shows a freshening at the surface in the seas surrounding the Indonesian Seas with a spatial pattern that resembles the surface freshwater flux (see Figure 5b of Durack & Wijffels, 2010). The upper thermocline water, on the other hand, shows a different spatial pattern (see Figure 10a of Durack & Wijffels, 2010). A salinity increase is observed in the source region of the ITF water, the region east of the Philippines, while freshening is observed in the exiting region, the Indo-Australian Basin. If the ITF simply advected water mass through the Indonesian Seas, salinity should increase in the Indo-Australian Basin. This freshening trend suggests an enhanced role of precipitated water through vertical mixing within the Indonesian Seas. Using a 1-D model, Phillips et al. (2005) find the observed interannual variability of the surface-to-subsurface salinity in the Indo-Australian Basin to be induced by the variability in precipitation over the Indonesian Seas. Zhang et al. (2016) find the importance of surface fluxes, entrainment, and advection from the Indonesian Seas by the ITF on the seasonal and interannual variability for the mixed layer salinity in the Indo-Australian Basin. Based on the salinity difference between the straits, Koch-Larrouy et al. (2008) suggest the fresh Java Sea water as the main source of the salinity changes that the ITF experiences within the Indonesian Seas although the source of this fresh Java Sea water is unclear.

The pathways of the precipitated freshwater from the Indonesian Seas to the Indian Ocean remain an open question. Precipitation and the flow field within the Indonesian Seas are strongly modulated by

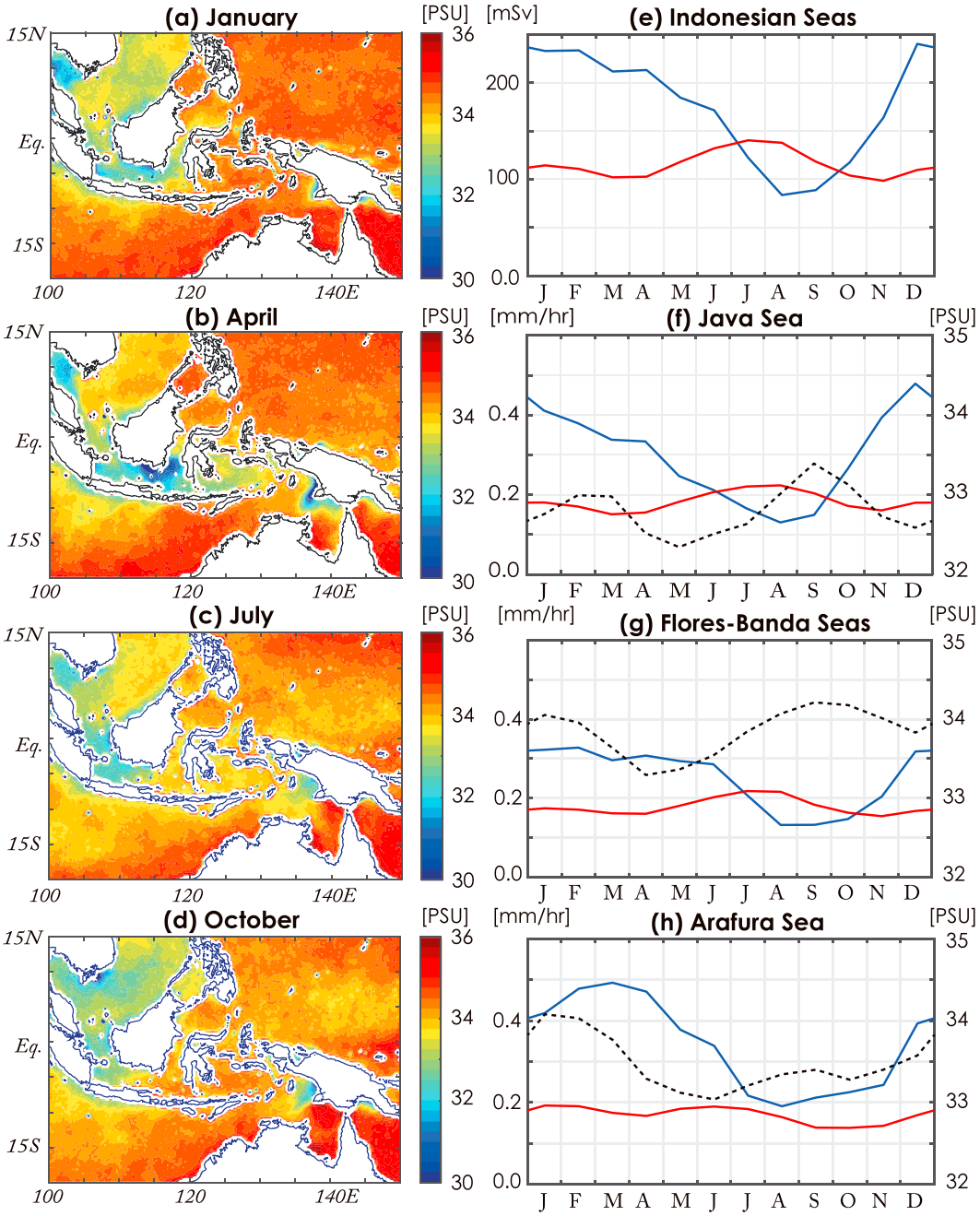

Figure 2. Observed monthly mean sea surface salinity based on Soil-Moisture Active Passion (SMAP) (2016–2017; Meissner & Wentz, 2016) for (a) January, (b) April, (c) July, and (d) October. (e) The seasonal cycle of precipitation (blue) and evaporation (red), integrated over the Indonesian Seas from OFES2. Local precipitation rate (blue), evaporation rate (red), and monthly mean sea surface salinity (black dashed) for (f) the Java Sea, (g) the Flores-Banda Seas, and (h) the Arafura Sea.

the monsoons, so these pathways are also likely to vary with season. The goal of this study is, therefore, to clarify the pathways of precipitated origin freshwater and its seasonal cycle. We will utilize a Lagrangian particle-tracking model and examine how the freshwater is modified as it disperses to the surrounding seas. The details of the numerical model will be described in section 2. The model results focusing on the dispersion due to lateral advection at the surface are presented in section 3, and the impact of evaporation, entrainment, and vertical mixing are presented in section 4. A summary is given in section 5.

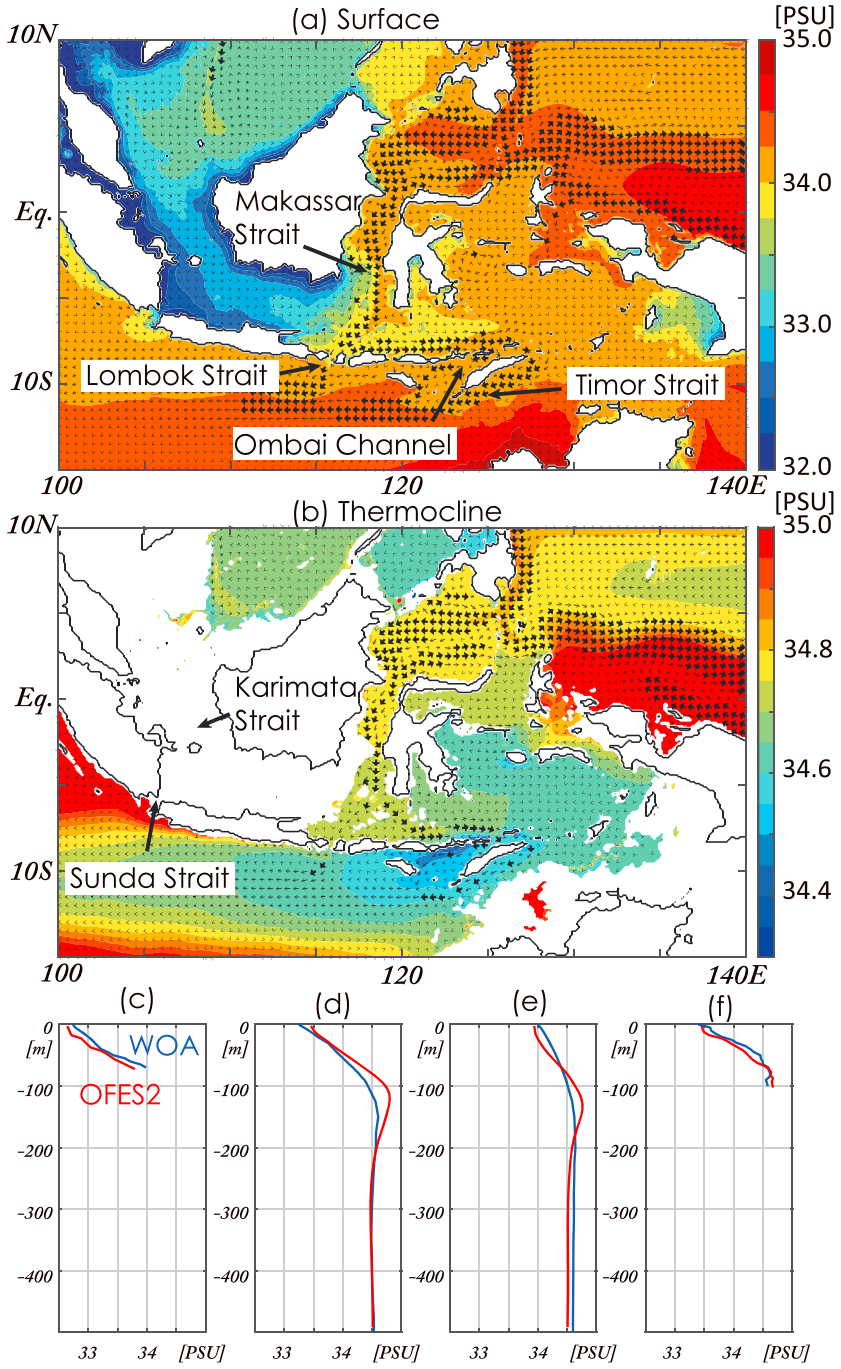

Figure 3. The climatological annual mean flow field in the Indonesian Seas from OFES2 (1995–2016) shown in vectors. (a) Vertical average from the surface to the depths of $\sigma_\theta = 23$ and (b) between $\sigma_\theta = 23$ and 26. Flow stronger than 20 cm/s are shown in bold, and salinity is shown in colors. Vertical profiles of the annual mean salinity in (c) the Java Sea (above −70 m), (d) the western Flores-Banda Seas, (e) eastern Flores-Banda Seas, and (f) the Arafura Sea. Blue lines are from WOA2013 (Boyer et al., 2013), and red lines are from OFES2.

2. The Model Setup

2.1. OFES2 Model Output

In order to estimate the trajectories of the Lagrangian particle tracking model, we use OFES2 from 1995 to 2016 (Sasaki et al., 2018). OFES2 is a quasi-global general circulation model that has a spatial resolution of 0.1° and is an update of OFES (Masumoto et al., 2004; Sasaki et al., 2008), which now includes a

global tidal mixing parameterization. Readers are referred to Sasaki et al. (2018) for model details. The 22-year monthly averaged OFES2 outputs are used to estimate the monthly climatologies, which are then used for the analysis unless noted otherwise.

The flow field and the water mass properties of the Indonesian Seas are found realistic and we consider the output appropriate for this study (Figures 3, 4b, and 4c). Near the surface, an eastward flow is forced during the northwestern monsoon season (Wyrtki, 1961) with a current along the northern coast of Nusa Tenggara that is associated with coastal upwelling (Kida & Wijffels, 2012; Wijffels et al., 2018). A northward current exists in the Maluku Sea, which is a return flow from the Indonesian Seas to the Pacific. A westward flow is forced during the southeastern monsoon season that is associated with upwelling in the Arafura Sea (Gordon & Susanto, 2001; Kida & Richards, 2009). The flow through the outflowing straits of the ITF also strengthens during this season (Sprintall et al., 2009). Salinity at the surface is similar to observations since it is restored to WOA2013 (Boyer et al., 2013) with a time scale of 15 days (Figure 3a). The vertical profiles in the Java Sea, the western part of the Flores-Banda Seas (115–123°E), the eastern part of the Flores-Banda Seas (123–133°E), and the Arafura Sea (Figures 3c–3f) are also well captured, although the stratification in the eastern part of the Flores-Banda Seas is somewhat stronger than observations.

2.2. Lagrangian Particle Tracking Model

2.2.1. Pathways of Precipitation Origin Freshwater

Connectivity Modeling System particle tracking model (Paris et al., 2013) is used to explore the pathways of precipitation origin freshwater of the Indonesian Seas. Particles are released only over these seas (Figure 4a), and they are advected horizontally based on the climatological monthly mean flow field of OFES2 as

$$\boldsymbol{x}(t+\Delta t) = \boldsymbol{x}(t) + \boldsymbol{u}\cdot\Delta t + \alpha\sqrt{2K_H\cdot\Delta t}, \tag{1}$$

where $\boldsymbol{x}$ is the location in longitude and latitude, $\boldsymbol{u}$ is the vertical average of the horizontal flow from the surface to $\sigma_\theta = 23$, and Δt is the time step set to 1 hr. The last term on the right-hand side (RHS) is a parameterization of the impact from eddies and flow variability by horizontal diffusion based on a random walk. K_H is the horizontal diffusivity coefficient set to 300 m^2/s, similar to that used in Kida and Wijffels (2012), and the model results are not overly sensitive to this value. Parameter α is a random number with a normal distribution. We chose $\sigma_\theta = 23$ to differentiate the surface water and the thermocline water since this isopycnal is close to the bottom of the mixed layer but does not outcrop within the Indonesian Seas. Koch-Larrouy et al. (2008) define $\sigma_\theta = 23$ as the isopycnal that separates the upper thermocline water to that below. Outcropping occurs occasionally along the southwestern coast of Nusa Tenggara when the Kelvin waves of the Indian Ocean induce upwelling. The daily averaged mixed layer depth is then used to define the bottom of the surface layer. However, such a region is limited in time and space, and moreover, our analyses focus on the fate of particles within the Indonesian Seas, not the outside, so this method does not significantly affect our results.

Our Lagrangian model releases and extracts particles to track the impact of precipitation origin freshwater and we will show how such a model can be created from the salinity balance equation. The salinity (S) balance equation of the surface layer with a thickness of H is (e.g., Halkides et al., 2011)

$$\frac{\mathrm{d}S_m}{\mathrm{d}t} = \frac{S_m}{H}(E-P) - \left(\frac{\Delta S}{H}\frac{\partial H}{\partial t} + \left\langle w\frac{\partial S}{\partial z}\right\rangle\right) - \frac{1}{H}\left(K_Z\frac{\partial S}{\partial z}\right)_{z=-H}. \tag{2}$$

S_m is the vertically averaged salinity of the surface layer. Angled brackets $\langle\rangle$ represent the vertical average within the surface layer. The first term on the RHS is the surface forcing term, where E is evaporation and P is precipitation. The second term is the entrainment term, where ΔS is defined as

$$\Delta \mathrm{S} = \begin{cases} S_m - S_{\mathrm{det}} & \text{when } \dfrac{\partial H}{\partial t} < 0 \\ 0 & \text{when } \dfrac{\partial H}{\partial t} = 0 \\ S_m - S_{\mathrm{ent}} & \text{when } \dfrac{\partial H}{\partial t} > 0 \end{cases}.$$

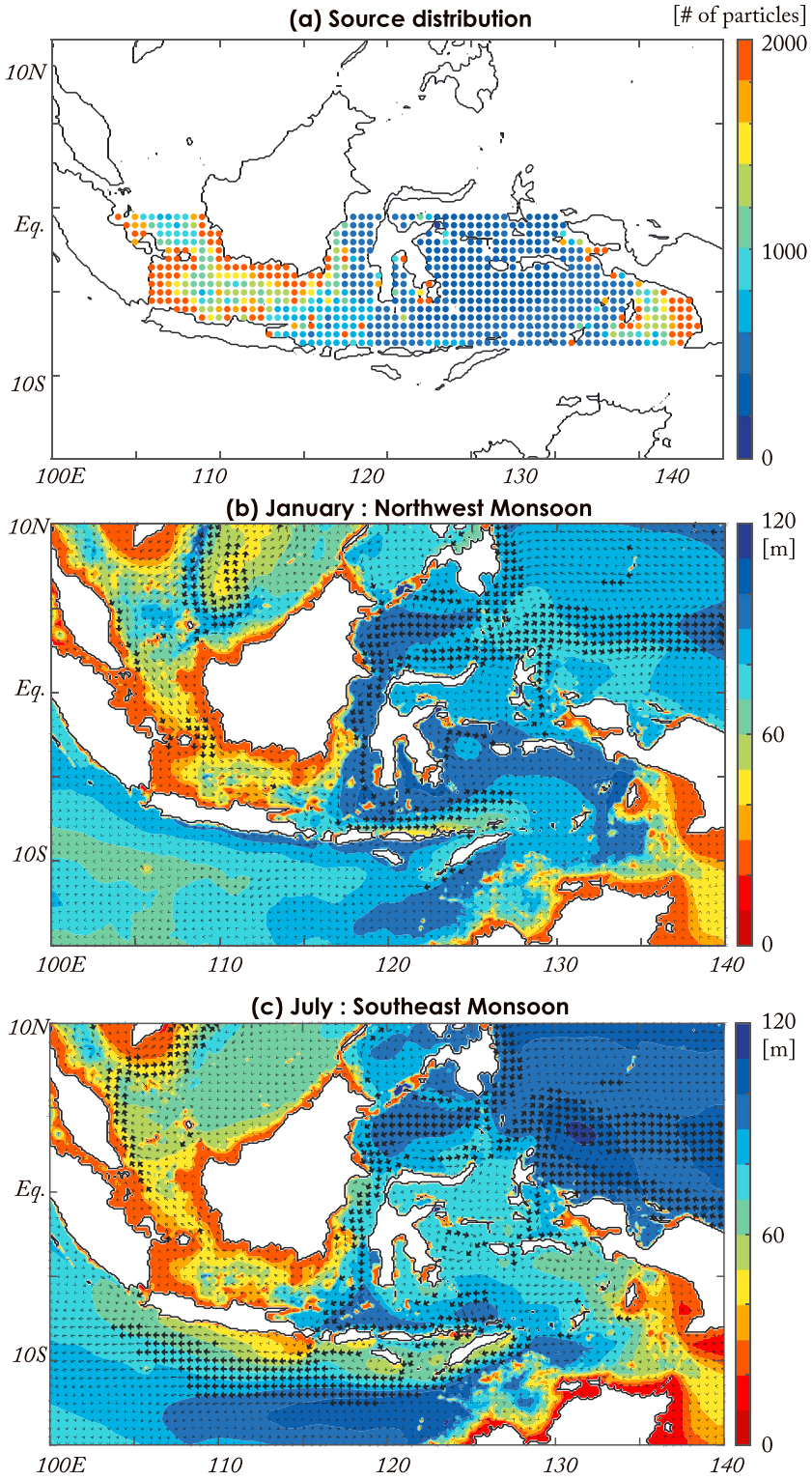

Figure 4. (a) The number of particles released on 1 January, shown every 0.5°. The monthly mean horizontal flow field (vector) and the depth of the surface layer (color) in (b) January and (c) July. Bold vectors are where the flow is stronger than 20 cm/s.

S_{det} and S_{ent} are salinity of the detrained and entrained water, respectively. If salinity within the surface layer is perfectly uniform in the vertical, S_{det} is equal to S_m and $\Delta S = 0$. The entrainment term can be expressed as $\frac{\Delta S}{H} w^*$, where w^* is the entrainment velocity (see Halkides et al., 2011, for details). The third term on the RHS of equation (2) is the vertical mixing term, where K_Z is the vertical diffusion coefficient and $\left(K_Z \frac{\partial S}{\partial z}\right)_{z=-H}$ is the vertical diffusive flux at the bottom of the surface layer. K_z varies in space and in time and the daily averaged diffusivity coefficient and salinity fields from the year 2016 will be used for estimating this term because we found monthly averaged outputs to overestimate the magnitude of highly time-varying mixing field.

We will define freshwater as $F = S_0 - S$, where S_0 is the reference salinity set to 35 psu, and focus on the freshwater anomaly created by precipitation rather than the mass. Equation (2) then becomes

$$\frac{dF_m}{dt} = \frac{S_0 - F_m}{H} P - \frac{S_0 - F_m}{H} E - \left(\frac{\Delta F}{H}\frac{\partial H}{\partial t} + \left\langle w \frac{\partial F}{\partial z} \right\rangle\right) - \frac{1}{H}\left(K_Z \frac{\partial F}{\partial z}\right)_{z=-H}, \tag{3}$$

where the subscripts represent the same definition as before. When representing F_m by the number of particles,F_m can be expressed as $\sum^N f_m$, where f_m represents the freshwater content of a particle within a volume and N is the number of particles. The RHS of equation (3) can be interpreted as source/sink terms, which would increase/decrease the number of freshwater particles following the flow.

Equation (3) can be further modified to focus on the precipitation origin freshwater (F_{mp}) from the rest (F_{mo}), that is, $F_m = F_{mp} + F_{mo}$. The first term on the RHS of equation (3) is precipitation and thus a source of F_{mp}. The rest of the terms are a source of freshwater if positive, but in such case, we will consider that they represent a source due to processes other than precipitation and thus a source of F_{mo}. The impacts of freshening due to entrainment/detrainment or reemergence of freshwater particles from the thermocline due to vertical mixing are thus not considered. If the terms are negative, they are a sink for both F_{mp} and F_{mo}, and if they affect F_{mp} and F_{mo} equally, changes in F_{mp} will occur based on its ratio $\gamma \left(= \frac{F_{mp}}{F_m}\right)$ so equation (3) can be rewritten for an equation for F_{mp}:

$$\frac{dF_{mp}}{dt} = \frac{S_0 - F_m}{H} P - \gamma \frac{S_0 - F_m}{H} E - \{\gamma, 0\}\left[\frac{\Delta F}{H}\frac{\partial H}{\partial t} + \left\langle w \frac{\partial F}{\partial z} \right\rangle\right] - \{\gamma, 0\}\left[\frac{1}{H}\left(K_Z \frac{\partial F}{\partial z}\right)_{z=-H}\right]. \tag{4}$$

The terms with curly brackets $\{A,B\}[C]$ represent A · C when C is positive but B · C when C is negative. Our Lagrangian particle tracking model will use equation (4) to track the pathways of precipitation origin freshwater. By evaluating the pathway of particles from source to sink, the fate of precipitated freshwater can be examined quantitatively from a Lagrangian framework.

2.2.2. The Source of Freshwater Particles

The source of F_{mp} is the first term of equation (4) and its increase over a period of τ can be estimated by releasing N_{mp} particles (Figure 4a), where

$$N_{mp} = \frac{\delta F_m}{f_w} = \frac{(S_0 - F_m)\cdot P}{H \cdot f_w}\tau. \tag{5}$$

δF_m is the increase in freshwater and f_w is the freshwater content of each particle, which we will set to 2×10^{-4} psu. This roughly corresponds to a release of 500 particles to represent a change in freshwater due to a weak 0.2-millimeter/hr rainfall over a water column of 50 m and salinity of S_0 ($F_m = 0$) for a month. N_{mp} is estimated every 0.1° each month, and we will assume that all monthly precipitation occurs on the first day (τ = 1 month). While the actual precipitation occurs over multiple weather events, we chose this approach since it is simple and useful for distinguishing the roles of source and sinks. As we will describe later, the model results remain qualitatively similar even when constant rainfall is used throughout the month. We also decided to estimate N_{mp} using P instead of $P - E$, because even a moderate surface mixing of $K_V = 1 \times 10^{-3}$ m^2/s can redistribute precipitated water across the surface layer in less than a day. This is much shorter than a month, which we use to estimate N_{mp}, so the freshwater that evaporates are not necessarily the same as the freshwater that precipitated.

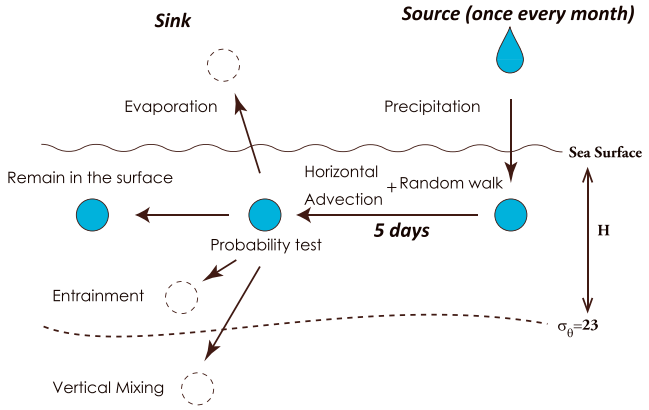

Figure 5. A schematic of the Lagrangian particle tracking model for tracking precipitation origin freshwater. Freshwater particles are added each month where precipitation occurs (source). These particles are then advected horizontally for 5 days by the monthly mean flow plus a random walk. The fate of each particle is then determined based on the probability test. Particles either remain in the surface layer or extracted due to evaporation, entrainment, or vertical mixing.

2.2.3. The Sink of Freshwater Particles

The evaporation, entrainment, and vertical mixing terms on the RHS of equation (4) become the sink terms when they are negative. The evaporation term is always present because E is positive by definition. The entrainment term is present only during entrainment $\left(w>0 \text{ and } \frac{\partial H}{\partial t}>0\right)$ for the Indonesian Seas because the surface layer is generally fresher than the subsurface $\left(\Delta F>0 \text{ and } \frac{\partial F}{\partial z}>0\right)$. The vertical mixing term is also mostly present since K_z is positive and the surface layer in the Indonesian Seas is, again, generally fresher than the subsurface $\left(\frac{\partial F}{\partial z}>0\right)$.

A sink of F_{mp} corresponds to an extraction of particles, and we will simulate this extraction based on freshwater balance. For example, if the freshwater balance equation suggests a 20% decrease in freshwater within a volume, 20% of particles that existed in this volume will be extracted with the particles chosen randomly. The rate of decrease in F_{mp} over a period of ΔT can be derived from equation (4) as

$$\frac{\Delta F_{mp}}{F_{mp}} = -\frac{\Delta T(S_0-F_m)}{F_m \quad H}E-\frac{\Delta T}{F_m}\cdot\left(\frac{\Delta F\partial H}{H \ \partial t}+\left\langle w\frac{\partial F}{\partial z}\right\rangle\right)-\frac{\Delta T}{F_m}\cdot\left(\frac{1}{H}\left(K_z\frac{\partial F}{\partial z}\right)_{z=-H}\right) \quad (6)$$
$$= -\text{Sink}_e-\text{Sink}_a-\text{Sink}_d \quad .$$

Sink_e, Sink_a, and Sink_d represent the probability of decrease due to evaporation, entrainment, and mixing, respectively, and the magnitude of these terms can be estimated from OFES2 output. Equation (6) expresses the probability of particles extracted by each process so the fate of each particle can be simulated by generating a random number R between 0 to 1 for every particle per ΔT and determining the fate by

$R \leq \text{Sink}_e$	Lost to evaporation
$\text{Sink}_e < R \leq \text{Sink}_e + \text{Sink}_a$	Lost to entrainment
$\text{Sink}_e + \text{Sink}_a < R \leq \text{Sink}_e + \text{Sink}_a + \text{Sink}_d$	Lost to vertical mixing
$\text{Sink}_e + \text{Sink}_a + \text{Sink}_d < \text{R}.$	Remains within the layer

We will refer to this procedure as the probability test.

2.2.4. Time Integration and the Basic Model Setup

Time integration proceeds in five steps (Figure 5). (Step 1) Release N_{mp} particles once a month based on equation (5). (Step 2) Particles are advected for 5 days based on equation (1). (Step 3) The magnitude of the sink terms in equation (6) are estimated for each particle ($\Delta T = 5$ days). (Step 4) A random number is generated, and the fate of each particle is determined based on the probability test. (Step 5) If the particle is decided to remain within the surface layer, repeat from Step 2. If not, then extract the particle from the model and time integration for this particle ends. With these time stepping procedures and enough particles to express the magnitude of the sink terms, we now have a Lagrangian model that can track the fate of precipitation origin freshwater.

Particles are released from January to December within the Indonesian Seas and their trajectories are calculated for a year. Particles released between 105–115°E, 115–133°E, and 133–140°E within 8°S to equator are defined as the Java Sea, Flores-Banda Seas, and Arafura Sea origin freshwater, respectively (Figures 1 and 4a). Model results are not overly sensitive to the detailed specification of the boundaries. Past studies using a Lagrangian model for understanding salinity changes in the Indonesian Seas focused on the changes in SSS (Miyama et al., 1996) or changes in water mass properties of the ITF following the flow from the North Pacific to the Indian Ocean (Koch-Larrouy et al., 2008). By following a water parcel, these studies can teach us how changes in salinity and freshwater occur but the knowledge about the source becomes ambiguous

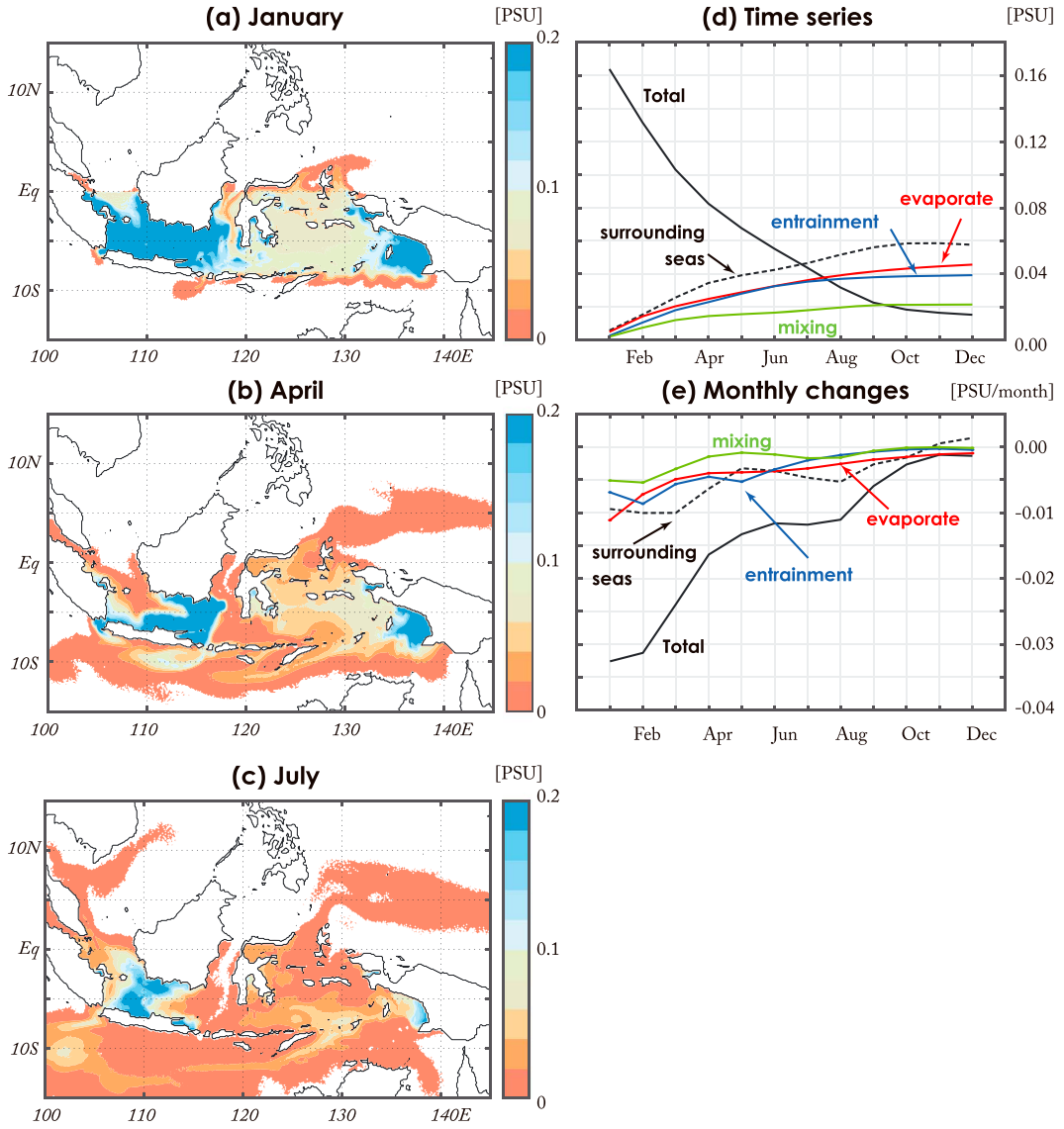

Figure 6. The monthly averaged distribution of particles in the surface layer for (a) January, (b) April, and (c) July that are released on 1 January. (See text for conversion between practical salinity unit and particle numbers.) (d) The number of particles that entered in January and (e) its tendency over the Indonesian Seas. The total number of particles within the Indonesian Seas is in black. The accumulated sum of particles lost to advection, evaporation, entrainment, and vertical mixing are in dashed black, red, blue, and green, respectively.

when the water parcel is affected by other sources since it is only the mean property that is tracked. By resolving the pathways of precipitation origin freshwater from different sources throughout its trajectory, the current approach enables us to differentiate the roles of freshwater of the Indonesian Seas from different areas and seasons.

3. The Dispersion of Particles at the Surface

3.1. Model Results

Once particles are released, they are advected around the Indonesian Seas and begin to escape to the SCS, the Pacific Ocean, and the Indian Ocean. We will first show the distribution of particles released on 1 January, which is the middle of the northwest monsoonal season and when a large input of freshwater occurs (Figures 2a and 2e). Most particles are still within the Indonesian Seas for the first month (Figure 6a), but

after a few months, some begin to escape to the surrounding seas (Figures 6b and 6c). Note that the number of particles is converted to the corresponding magnitude in freshwater in the figures hereafter. Gradual decay in the total number of particles is also observed because some of the particles are lost to evaporation, entrainment, and vertical mixing. The magnitude of these sinks based on equation (6) suggests a monthly decrease of about 14% over the Indonesian Seas on a spatial average, which matches well with the model result (Figures 6d and 6e). Precipitation origin freshwater decays exponentially in about 6 months, where 34% is due to advection to the surrounding seas, 26% is due to evaporation, 26% is due to entrainment, and 13% is due to vertical mixing.

The ITF and the monsoonal wind-driven surface flow are the primary agents for advecting the freshwater particles. In January, most particles are advected by the eastward flow that is driven by the northwestern monsoon. The freshwater maximum of the Java Sea thus shifts to the east (Figure 6a). Particles disappear where inflow from the surrounding seas occur, such as the Karimata and Makassar Straits, because we are only tracking the Indonesian Seas origin freshwater. Particles in the Flores-Banda Seas and the Arafura Sea converge near the coastline of New Guinea due to the northeastward Ekman flow.

In April, advection by the ITF establishes a region with only a few particles from the Makassar Strait to the northern coast of Nusa Tenggara (Figure 6b). The distribution of particles in the Indonesian Seas is thus separated to that in the Java Sea and that in the Banda and Arafura Seas. For the Java Sea, the number of particles changes abruptly near the shelf break between the Flores Sea, while advection of the SCS water is observed in the west. Particles in the Java Sea appear to exit to the Indian Ocean through the Sunda and Lombok Straits, creating plume-like features on the Indian Ocean side of the straits. For the Banda-Arafura Seas, the number of particles increases toward the east but some of the particles escape to the west through the Timor Strait to the Indian Ocean. This signal is, however, weak compared to that through the Lombok Strait, creating a strip-like signal rather than a plume. We also find some particles escaping to the Pacific Ocean through the Maluku Sea to join the North Equatorial Countercurrent.

In July, the freshwater signal in the Indonesian Seas is significantly weaker. The majority of the particles left are found in the western Java Sea and the Arafura Sea with some remaining near the Ombai Channel and Timor Strait (Figure 6c). Stronger signals remain in the shallow seas where the impact of entrainment and vertical mixing is absent, and evaporation is the only sink. Particles shift to the west of the Java Sea because of the westward flow driven by the southeast monsoonal wind (Figure 6b), with some particles entering the interior of the SCS. Particles disappear on the eastern side of the Java Sea due to the intrusion of the Flores Sea water. We find particles exiting to the Indian Ocean through the Sunda Strait, Ombai Channel, and Timor Strait, but not much through the Lombok Strait because it is, again, the Flores Sea water that is exiting through this strait. A freshwater lens, centered around 10°S and 102°E, is created by the particles that exited the Lombok Strait in spring (Figure 6c). Particles exiting through the Ombai Channel and Timor Strait appear to be those that existed in the Banda-Arafura Seas in spring, which is then advected southwestward by the surface Ekman flow in summer.

We find the results qualitatively similar when particles are released daily (Figure S1 in the supporting information) instead of the first day (Figure 6). The number of particles increases about 10% for those released daily with the secondary peak of advection to the surrounding seas in July instead of August. Nonetheless, the exponential decay of about 6 months is observed and the impact of the sinks remain the same. As a result, the distribution of the particles in April and October is also similar.

Particles that are released in other months are similarly advected by the ITF and the monsoonal wind-driven flow field (not shown) with a gradual decay in the number of particles occurring in about 5–6 months. Major differences arise due to the direction of the monsoonal wind-driven flow when the particles are released. We will examine how the seasonal cycle in the movement of these particles affect the properties at the outflow straits in more detail later.

3.1.1. The Sum of Precipitation Origin Freshwater

The sum of all freshwater particles released from August to July that existed on 31 July is shown in Figure 7a. This distribution shows the sum of the freshwater signal created by precipitation that occurred within a year. We find the spatial pattern of the freshwater signal resembling that of observed SSS in July (Figure 2c). Observed SSS in the Java Sea is about 32.5 psu, whereas that in the Flores Sea is about 33.5 psu, so the magnitude of the spatial differences is also comparable. This suggests that precipitation is

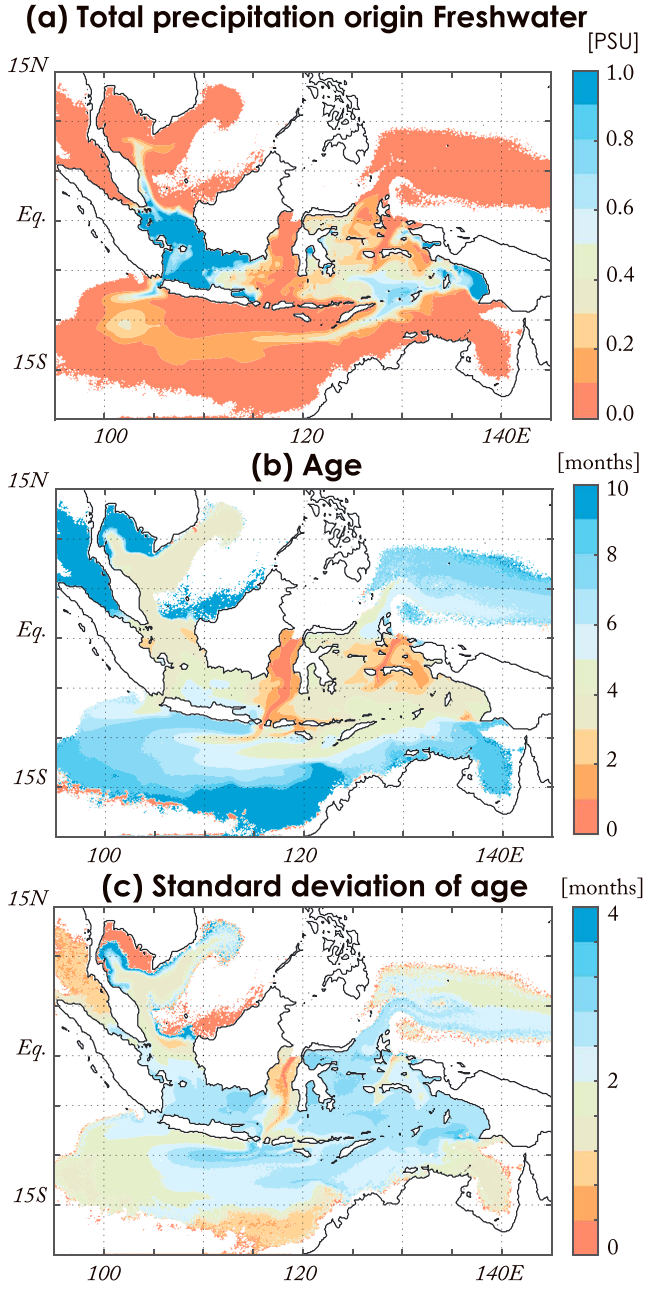

Figure 7. (a) The distribution of particles in the surface layer on 31 July due to particles released from August (prior year) to July. (See text for conversion between practical salinity unit and particle numbers.) (b) The average age and (c) its standard deviation for particles shown in (a).

responsible for creating the SSS spatial pattern that establishes within the Indonesian Seas, and it is the precipitation that occurs within a year rather than an accumulation over many years. Considering that surface freshwater signals decay exponentially in about 6 months (Figure 6d), it is the precipitation that likely occurred within 6 months that is mainly responsible. There are, however, differences. Our model results show a moderate freshwater signal near the Ombai Channel and Timor Strait, but such a feature is not found in the observed SSS. Since our model reflects changes in freshwater only due to precipitation origin, the difference suggests the impact of changes occurring in the background freshwater field or river run-off.

3.1.2. Age of the Freshwater Particles and Its Variance

The age of particles can be defined as the residence time in the surface layer from the time of release. By estimating the age for all the particles that were released from August to July that existed on 31 July (Figure 7a), we find the average age of particles in the Indonesian Seas to be about 4 months (Figure 7b). This matches well with the 6-month exponential decay of particles from the surface (Figure 6d). Young particles are found near the Makassar Strait and the Halmahera Sea, where the number of particles is also small. These regions are where the flow quickly advects particles elsewhere and old particles do not exist. The variance of particle age confirms the small variance in age over this region (Figure 7c). Old particles are found in the southern half of the Java Sea where the age is about 5–6 months. This suggests the presence of particles that entered the Indonesian Seas from January to February, which is precipitated water from the northwestern monsoon season. The large variance in age also suggests that freshwater in this region consists of particles that entered in various months.

For particles escaping to the Indian Ocean, youngest particles are found near the Lombok Strait where the ITF advects freshwater of the Indonesian Seas to the Indian Ocean. The majority of these particles escaping through the outflowing straits are about 3–4 months old when they exit. The variance also suggests that this outflow consists of particles with relatively large variance in age, suggesting that these particles include those that are accumulated over some period. In the surrounding seas, old particles are found near the coast of SCS and along the coast from the southern Arafura Sea to the northwestern shelves of Australia. However, the number of particles in these regions is small and has small variance in age (Figures 7a and 7c).

3.2. Pathways to the Indian Ocean

Among the four outflowing straits, the major exports are those through the Lombok and Timor Straits and they occur with a large seasonal cycle (Figures 8a–8d). The seasonal cycle at the Sunda Strait is moderate with a minimum from November to December (Figure 8a). Larger mass transport occurs in the southeastern monsoon season (Susanto et al., 2016), but because the Java Sea is fresher during the northwestern monsoon season, the seasonal cycle of the freshwater flux appears to become moderate. Particles that exit through the Sunda Strait originate from the Java Sea. The seasonal cycle at the Lombok Strait shows a maximum during the northwestern monsoon season (Figure 8b) when the fresh Java Sea water reaches the Flores Sea and the Lombok Strait. Once the particles enter the ITF, they are quickly advected to the Indian Ocean through the Lombok Strait. Particles that exit through the Lombok Strait are Java Sea origin, while those from the rest of the Flores-Banda Seas are secondary. The Flores-Banda Seas origin particles are also those from around the Makassar Strait rather than the rest of the Flores-Banda Seas.

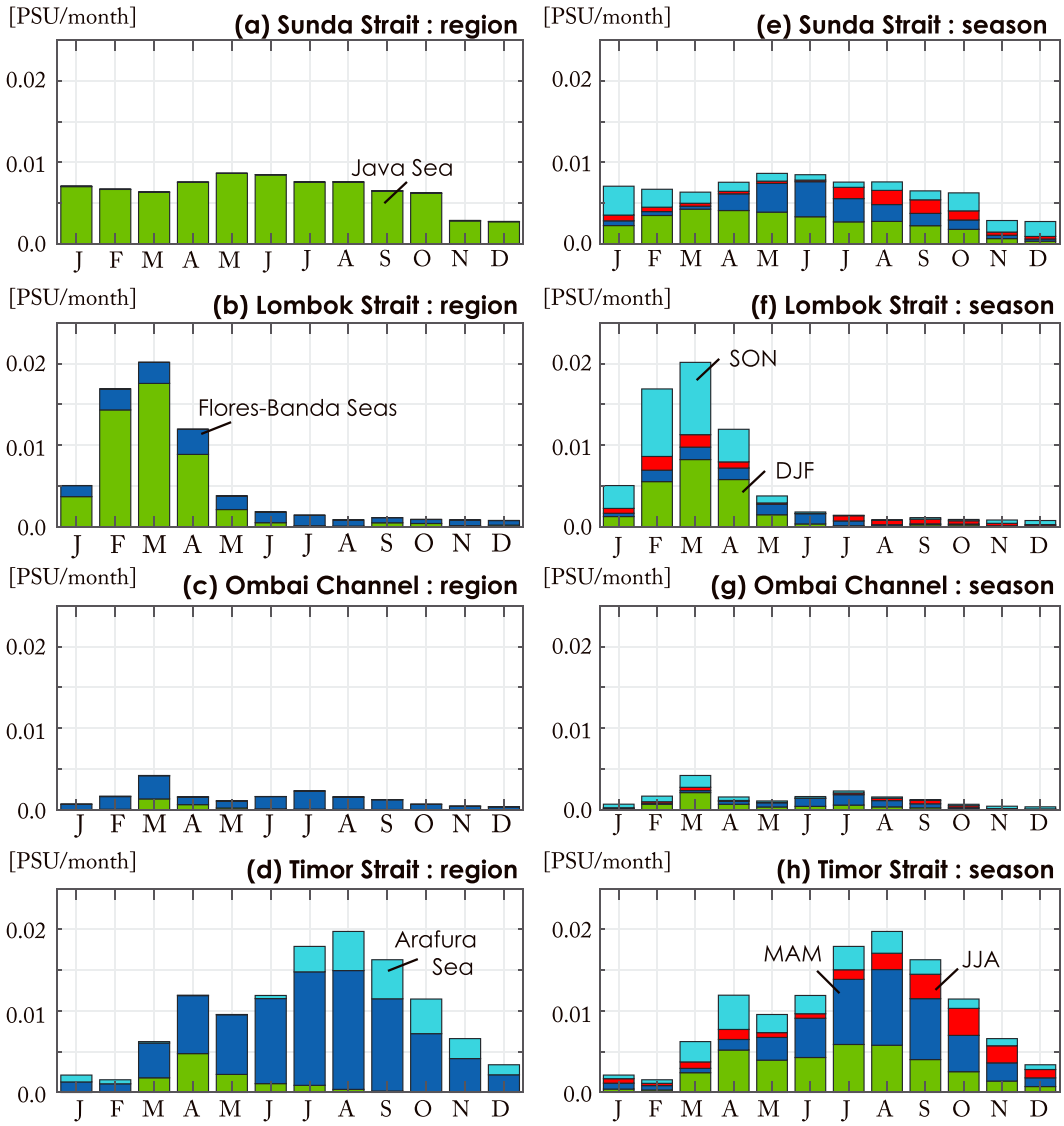

Figure 8. Monthly histograms of the number of particles that exit to the Indian Ocean from (a) the Sunda Strait, (b) Lombok Strait, (c) Ombai Channel, and (d) Timor Strait. (See text for conversion between practical salinity unit and particle numbers.) Particles that originate from the Java Sea (green), Flores-Banda Seas (blue), and the Arafura Sea (cyan) are shown colors. (e–h) Same as (a)–(d) but the colors represent particles from precipitation during DJF (green), MAM (blue), JJA (red), and SON (cyan). SON = September–November; DJF = December–February; MAM = March–May; JJA = June–August.

The seasonal cycle at the Ombai Channel shows a maximum in March and a secondary maximum in July (Figure 8c). This secondary maximum matches with when the maximum mass transport occurs due to the southwestward Ekman flow (Sprintall et al., 2009). The maximum in March, therefore, is likely a result of enhanced freshening due to the advection of from the west. The Java Sea origin particles are indeed observed at the strait in March. The seasonal cycle at the Timor Strait shows a maximum in August and a secondary maximum in April (Figure 8d). The majority of the particles are Flores-Banda Seas origin, but the secondary maximum in April appears to be associated with the advection from the west, like the maximum observed at the Ombai Channel in March. The maximum in August matches with when enhanced transport occurs due to the surface Ekman flow. Another difference from the Ombai Channel is that the Arafura Sea origin particles are observed from late summer to fall. This confirms the pathway for the Arafura Sea precipitated freshwater exiting to the Indian Ocean through this strait as observed in Figure 6b.

The Lagrangian model can also determine when the particles entered the Indonesian Seas. For the Sunda Strait outflow, particles that entered during the maximum precipitation season (December–February,

DJF) contribute the largest (Figure 8e). The peak of DJF precipitated freshwater is found in March, reflecting the signal accumulating in time. This is consistent with the fact that the source for the Sunda Strait outflow is the local Java Sea precipitated freshwater. For the Lombok Strait outflow, particles that entered in September–November (SON) and DJF contribute the most with both contributing equally at the time of maximum outflow in March (Figure 8f). This is because the source for the Lombok Strait outflow is the Java Sea. Large contribution from SON precipitated freshwater reflects the advection time required for the particles to reach the strait. For the Ombai Channel and Timor Strait outflows, particles that entered in DJF and March–May (MAM) contribute the most (Figures 8g and 8h). These seasons are when local precipitation is strong (Figure 2g), which suggests that the particles reside in the surface of the Flores-Banda Seas for a few months before exiting to the Indian Ocean.

When integrated over all four straits, about 50%, 42%, and 8% of the particles exiting to the Indian Ocean originate from the Java Sea, Flores-Banda Seas, and the Arafura Sea, respectively. The Java Sea and the Flores-Banda Seas origin particles contribute roughly with about the same magnitude. The model also shows 35%, 27%, 13%, and 25% of these particles entered the Indonesian Seas during DJF, MAM, June–August (JJA), and SON, respectively. Precipitation during DJF contributes the most, while those from JJA is the weakest. This matches well with the seasonal cycle of the total freshwater input (precipitation minus evaporation) that the Indonesian Seas receive (Figure 2e).

4. Impact of Evaporation, Entrainment, and Vertical Mixing

As the precipitation origin freshwater disperses to the surrounding seas near the surface, some are also lost due to evaporation, entrainment, and vertical mixing (Figure 6d). An exponential decrease occurs in about 6 months, and for particles released on 1 January, we find 34% of the decrease due to lateral advection to the surrounding seas and 66% of the decrease due to the freshwater sinks. The number of particles released in April, July, and October shows similar exponential decay in time, but there are differences in monthly tendencies, and they tend to enhance during January–February and July–August (Figure 6e). Part of this semiannual signal is due to lateral advection, but similar signal is also found in the freshwater sinks, especially vertical mixing. The semiannual signal suggests the role of the monsoonal winds, as January–February and July–August correspond to the peak of the northwestern and southeastern monsoonal winds, respectively.

4.1. Evaporation

As equation (6) shows, the magnitude of the evaporation term depends on the evaporation rate, surface freshwater, and thickness of the surface layer. The seasonal cycle of the evaporation rate over the Indonesian Seas shows a maximum from July to August, but the magnitude of this seasonal cycle is relatively moderate compared to precipitation (Figure 2e). The impact of evaporation on freshwater does not change much throughout the year.

The spatial variability in the magnitude of the evaporation term reflects the differences in the surface layer depth and surface freshwater (Figure 9a). The spatial variability associated with the evaporation rate is weak. Larger impact is found in the shallow seas, such as the Java Sea and the Arafura Sea, compared to the deeper Flores-Banda Seas. The spatial variability associated with surface freshwater tends to work in the opposite sense because fresher surface water in the shallow seas reduces the magnitude of the evaporation term (Figure 7a). Nonetheless, its impact appears weak and we find the magnitude of the evaporation term strongest in the shallow seas. The role of evaporation found along 12°S in the Indian Ocean is a result of the ITF advecting particles zonally along this latitude rather than the spatial variability in salinity, surface layer depth, or evaporation.

4.2. Entrainment

Entrainment of saltier subsurface water results in loss of freshwater particles for the surface layer, and this impact is found to be associated with significant spatial variability (Figure 9b). The location of entrainment is localized in space and is found in narrow strips where abrupt changes in topography occur, such as those near the coast and shelf breaks. Large values are found along the shelf break between the Java Sea and the Flores Sea and along the northern coast of Nusa Tenggara. The shelf breaks between the Banda Sea and the Arafura Sea and along the southern coast of New Guinea are another location with large values.

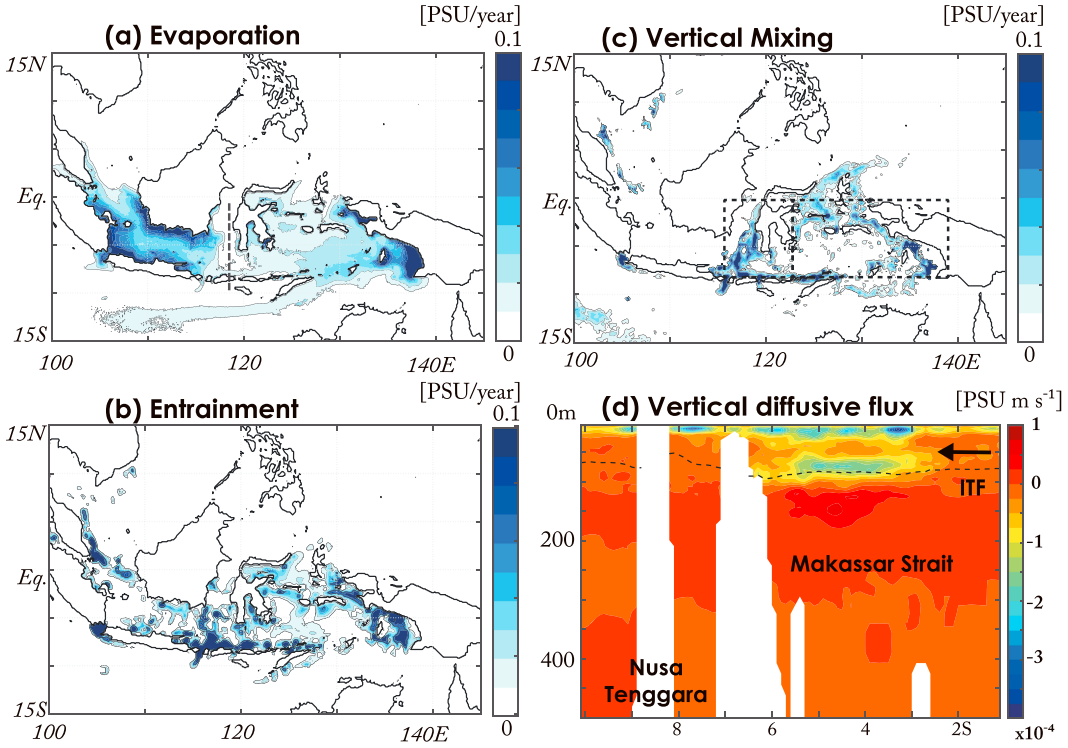

Figure 9. Annually integrated number of particles lost to (a) evaporation, (b) entrainment, and (c) vertical mixing. (See text for conversion between practical salinity unit and particle numbers.) The dashed boxed lines show where we define as the west and east in Figure 10. (d) The meridional cross section of the vertical diffusive flux ($K_z \frac{\partial S}{\partial z}$) across the Makassar Strait (dashed line in panel a). The dashed line indicates the depth of the surface layer.

These areas correspond to where upwelling events occur. The northwestern monsoonal wind induces upwelling along the northern coast of Nusa Tenggara in winter while the southeastern monsoonal wind induces upwelling in the northern Arafura Sea in summer.

The impact of entrainment on freshwater is also large on the Indian Ocean side of the Sunda Strait and the Lombok Strait. These signals are due to upwelling events induced by the Kelvin waves of the Indian Ocean when they propagate along the southern coast of the Java island. During these events, entrainment of subsurface Indian Ocean waters occurs at the Indian Ocean side of the strait, which reduces the freshwater signal. As a result, the freshwater signal at the straits significantly weakens on the Indian Ocean side of the straits.

4.3. Vertical Mixing

Vertical mixing occurs in similar regions as where entrainment occurs (Figure 9c). Larger values are found along the shelf break between the Java Sea and the Flores Sea, the northern coast of Nusa Tenggara, and the Makassar Strait. This is along the main route of the ITF. We also find larger values along the shelf break between the Banda Sea and the Arafura Sea, the southern coast of New Guinea, and the Halmahera Sea. This may affect the eastern route of the ITF. No impact is found in the shallow seas where water mass denser than $\sigma_\theta = 23$ does not exist. One of the major differences in the fate of freshwater due to entrainment and vertical mixing is that entrainment results in the disappearance of the freshwater signal within the layer while vertical mixing results in an exchange of water mass with the thermocline. Particles thus leave the surface layer and enter the thermocline for vertical mixing. While the impact on the total number of freshwater particles is smaller for vertical mixing compared to other sink terms (Figure 6d), this term is critical for allowing precipitation origin freshwater to enter the ITF thermocline.

When examining the Flores-Banda Seas separately across 125°E, we find 37% of vertical mixing occurring in the western part and 63% occurring in the eastern part (Figure 9c). Vertical mixing in the west occurs with a peak in February, while that in the east occurs with a peak in August. This results in a semiannual signal

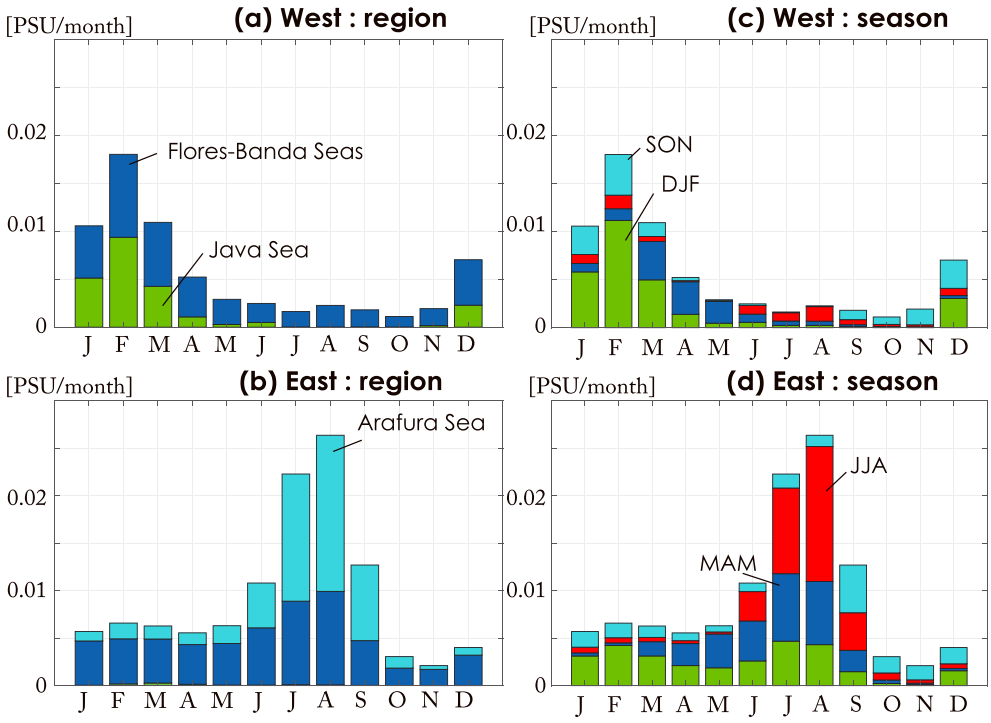

Figure 10. The monthly histogram of the number of particles that enter the thermocline due to vertical mixing in (a) the west and (b) the east for the region from the Flores-Banda Seas to the Arafura Sea (dashed boxes in Figure 9c). (See text for conversion between practical salinity unit and particle numbers.) Particles that originate from the Java Sea (green), Flores-Banda Seas (blue), and the Arafura Sea (cyan) are shown colors. (c, d) Same as (a) and (b) but the colors represent particles from precipitation during DJF (green), MAM (blue), JJA (red), and SON (cyan). SON = September–November; DJF = December–February; MAM = March–May; JJA = June–August.

when integrated over the whole Indonesian Seas, which explains how the semiannual signal found in the monthly tendencies occur (Figure 6e). The mechanism behind the seasonal cycle in vertical mixing is likely the monsoonal wind-induced upwelling, the same as that behind entrainment. During the upwelling season, the surface layer depth becomes shallow so that the impact of vertical mixing enhances.

The origin of the particles entering the thermocline in the eastern part of the Flores-Banda Seas is found to be local, from the Flores-Banda Seas and the Arafura Seas (Figure 10b). Those from the Arafura Sea shows a stronger seasonal cycle than that from the Flores-Banda Seas. The origin of particles entering the thermocline in the western part, on the other hand, appears to be more nonlocal (Figure 10a). About 35% of the particles are from the Java Sea and these particles are associated with a large seasonal cycle and a peak in February. The number of particles from the Flores-Banda Seas has a weaker seasonal cycle. When examining the origins of these particles in more detail, we find them to come from the upstream region of the Makassar Strait. This is where the ITF advects the particles into the Indonesian Seas and since vertical mixing is enhanced along the Makassar Strait (Figure 9d), these particles leave the surface layer to the thermocline soon after they enter the strait.

Among the particles that enter the thermocline in the eastern part of the Flores-Banda Seas, we find maximum from those released during JJA (Figure 10d). This is later than the seasonal dependence found in the outflows through the Ombai Channel and the Timor Strait at the surface (Figure 8h), where the largest fraction was found to be those released during DJF and MAM. The difference is likely because vertical mixing can work directly when precipitation occurs. Among the particles that enter the thermocline in the western part of the Flores-Banda Seas, we find maximum from those released during DJF (Figure 10c). This is similar to the seasonal dependence found in the outflows through the Lombok Strait at the surface (Figure 8f). The importance of precipitation in winter reflects the seasonal precipitation cycle in the Java Sea, where maximum occurs in December (Figure 2b), and the time required for this signal to accumulate and be advected.

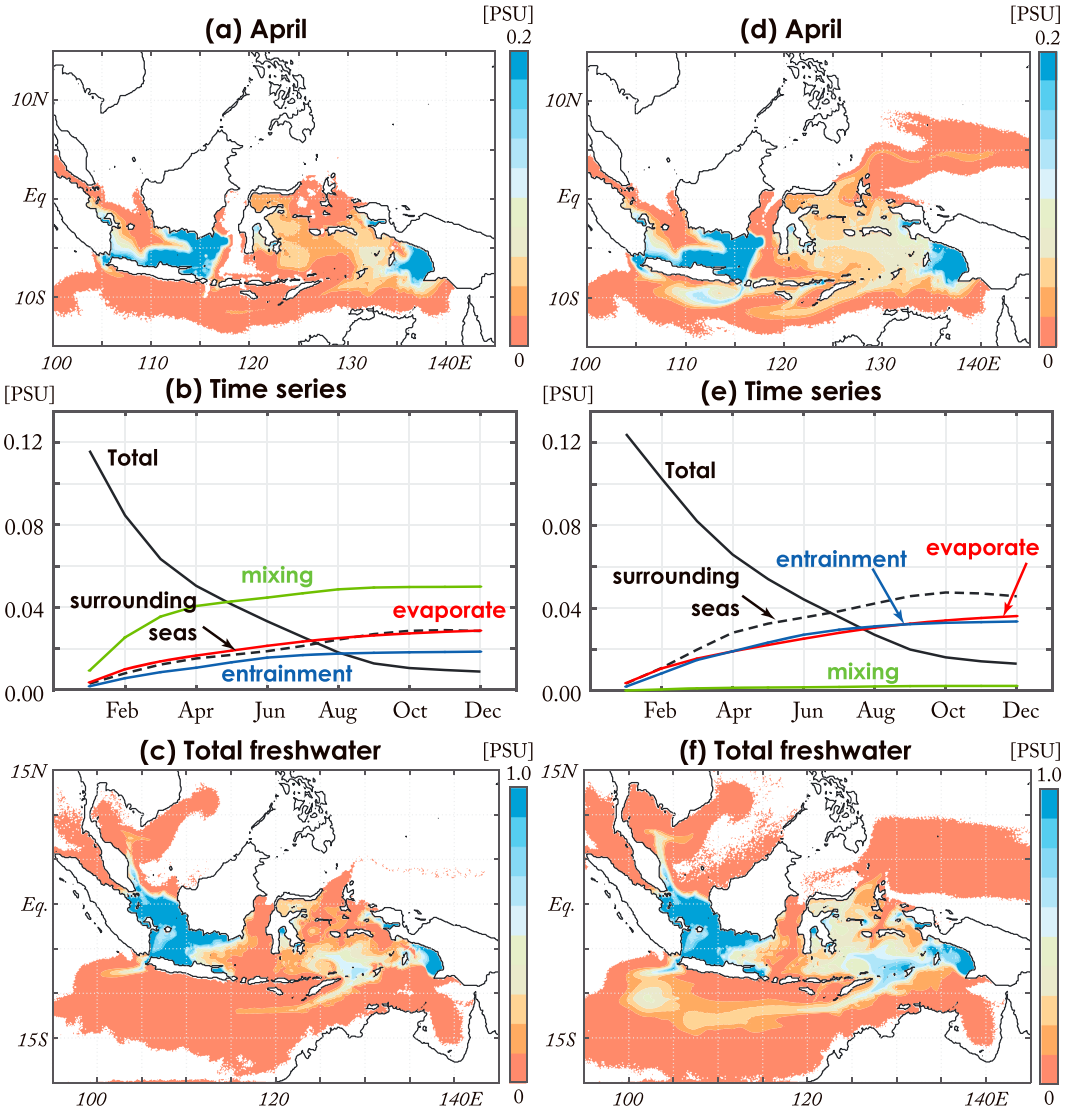

Figure 11. Model results when K_z is (a–c) 10 times larger and (d–f) 10 times smaller. (a, d) The distribution of particles in the surface layer for April that are released on 1 January. (See text for conversion between practical salinity unit and particle numbers.) (b, e) The number of particles within the Indonesian Seas and the accumulated sum of particles lost to advection, evaporation, entrainment, and vertical mixing, as in Figure 6d. (c, f) Total precipitation origin freshwater in the surface layer on 31 July due to particles released from August (prior year) to July as in Figure 7a.

4.3.1. Sensitivity to the Vertical Diffusivity Coefficient

How sensitive are the model results to the magnitude of K_z? When K_z is increased ten times, the surface residence time shortens, as expected, by about a month (Figure 11b). The role of vertical mixing enhances significantly, especially for the first few months, and becomes the primary sink of surface freshwater. With less particles at the surface, the relative roles of lateral advection to the surrounding seas and entrainment reduce. The freshwater signal in the Flores-Banda Seas reduces more quickly and the plumes of freshwater entering the Indian Ocean through the straits disappear (Figure 11a). The impact of evaporation does not change much because it occurs primarily over the shallow seas where vertical mixing is absent. Similar changes are found for the sum of all freshwater particles released from August to July on July 31 (Figure 11c). A reduction of freshwater is observed in the interior of the Flores-Banda Seas with less dispersion to the surrounding seas. Another notable aspect is that the difference between the shallow and deep seas increases.

Opposite changes are found when K_z is decreased ten times. The role of vertical mixing becomes negligible throughout the year and over most areas of the Indonesian Seas (Figure 11e). The freshwater signal within the Flores-Banda Seas increases (Figure 11d) and the signal of the freshwater plume entering the Indian Ocean is stronger at the straits. The sum of all freshwater particles released from August to July on 31 July (Figure 11f) also shows a slight increase in freshwater signal in the interior of the Flores-Banda Seas and the dispersion to the surrounding seas, including the continuous strip of freshwater found along 12°S.

5. Summary

The goal of this study was to learn the fate of the precipitated water that enters the Indonesian Seas. These seas are located where one of the largest precipitation occurs around the globe while also acting as a gateway of the water mass exchange between the Pacific and the Indian Ocean, known as the ITF. We utilized a Lagrangian particle tracking model that can track the dispersion of precipitation origin freshwater. Following the salinity balance equation at the surface, particles are released over the Indonesian Seas based on the intensity of precipitation (equation (5)) and extracted (equation (6)) based on evaporation, entrainment, and vertical mixing.

Our findings can be summarized as follows.

1. Once precipitated water enters the Indonesian Seas, its signal remains near the surface for about 6 months. The primary cause behind the loss of this freshwater signal is advection to the surrounding seas near the surface, followed by evaporation, entrainment, and vertical mixing.
2. Near the surface, the Java Sea precipitated freshwater and the Flores-Banda Seas precipitated freshwater exit to the Indian Ocean by roughly the same amount. The majority of the Java Sea precipitated freshwater exits through the Lombok Strait in late winter, and this freshwater is that accumulated from fall to winter. The majority of the Flores-Banda Seas precipitated freshwater exits through the Timor Strait in late summer to fall, and this freshwater is that accumulated from winter to spring.
3. Freshwater enters the ITF thermocline in narrow regions along shelf breaks and coastlines during the monsoonal wind-driven upwelling seasons. The Java Sea precipitated freshwater in winter enters the thermocline along the main route of the ITF. The Flores-Banda Seas precipitated freshwater in summer enters the thermocline along the eastern route of the ITF.

We have focused on the fate of precipitation origin freshwater for the climatological seasonal cycle in this study and so the impact of riverine freshwater remains an open question. There are many rivers surrounding the Indonesian Seas, but the monthly discharge rates from these rivers are still poorly known. Riverine freshwater will affect the surface salinity near river mouths, but how much they disperse to the interior of the Indonesian Seas needs further investigation. Precipitation also varies significantly in space and in time. This makes it difficult to capture and analyze its role from a Eulerian framework since the source region changes in time. A freshwater-tracking Lagrangian Model is a useful approach since the source of freshwater no longer need to be fixed in space, while the spatial distribution of freshwater can be simulated at the same time. A 2-D approach was taken in this study but a 3-D simulation that incorporates the impact of vertically varying vertical diffusivity could capture the fate of freshwater from the surface to depth more realistically. Although computationally more intensive, a surface layer depth need not be defined. The age and its variance also provide useful information when comparing with chemical tracers. Precipitation over the Indonesian Seas is known for its variability on intraseasonal and interannual time scales (Aldrian & Susanto, 2003) and how will these signals imprint on the ITF surface and thermocline water? We plan to examine these questions next.

Acknowledgments

S. Kida was supported by JSPS KAKENHI Grant Number JP18H03731. K. J. Richards was supported by NOAA by grant NA17OAR4310252. TRMM, SMAP, and WOA2013 data were downloaded from the APDRC website (http://apdrc.soest.hawaii.edu) and the Asia-Pacific Data Research Center of the University of Hawaii at Manoa. OFES2 output is available at the website (http://www.jamstec.go.jp/esc/fes/dods/OFES2). CMS particle tracking model was downloaded from the GitHub (https://github.com/beatrixparis/connectivity-modeling-system). This work was supported in part by the Collaborative Research Program of Research Institute for Applied Mechanics, Kyushu University.

References

Aldrian, E., & Susanto, R. D. (2003). Identification of three dominant rainfall regions within Indonesia and their relationship to sea surface temperature. *International Journal of Climatology*, *23*(12), 1435–1452. https://doi.org/10.1002/joc.950

Boyer, T. P., Antonov, J. I., Baranova, O. K., Coleman, C., Garcia, H. E., Grodsky, A., et al. (2013). In S. Levitus & A. Mishonov (Eds.), *World Ocean Database 2013, NOAA Atlas NESDIS* (Vol. 72, p. 209). Silver Spring, MD. https://doi.org/10.7289/V5NZ85MT

Dai, A., & Trenberth, K. E. (2002). Estimates of freshwater discharge from continents: Latitudinal and seasonal variations. *Journal of Hydrometeorology*, *3*(6), 660–687. https://doi.org/10.1175/1525-7541(2002)003<0660:EOFDFC>2.0.CO;2

Durack, P. J., & Wijffels, S. E. (2010). Fifty-year trends in global ocean salinities and their relationship to broad-scale warming. *Journal of Climate*, *23*(16), 4342–4362. https://doi.org/10.1175/2010JCLI3377.1

Fang, G., Qang, Y., Wei, Z., Fang, Y., Qiao, F., & Hu, X. (2009). Interocean circulation and heat and freshwater budgets of the South China Sea based on a numerical model. *Dynamics of Atmospheres and Oceans*, *47*(1-3), 55–72. https://doi.org/10.1016/j.dynatmoce.2008.09.003

Ffield, A., & Gordon, A. L. (1996). Tidal mixing signatures in the Indonesian Seas. *Journal of Physical Oceanography*, *26*(9), 1924–1937. https://doi.org/10.1175/1520-0485(1996)026<1924:TMSITI>2.0.CO;2

Gordon, A. (2005). Oceanography of the Indonesian Seas and their throughflow. *Oceanography*, *18*(4), 14–27. https://doi.org/10.5670/oceanog.2005.01

Gordon, A. L., & Susanto, R. D. (2001). Banda Sea surface-layer divergence. *Ocean Dynamics*, *52*(1), 0002–0010. https://doi.org/10.1007/s10236-001-8172-6

Halkides, D., Lee, T., & Kida, S. (2011). Mechanisms controlling the seasonal mixed-layer temperature and salinity of the Indonesian seas. *Ocean Dynamics*, *61*(4), 481–495. https://doi.org/10.1007/s10236-010-0374-3

Held, I. M., & Soden, B. J. (2006). Robust responses of the hydrological cycle to global warming. *Journal of Climate*, *19*(21), 5686–5699. https://doi.org/10.1175/JCLI3990.1

Huffman, G. J., Adler, R. F., Bolvin, D. T., & Nelkin, E. J. (2010). The TRMM Multi-satellite Precipitation Analysis (TMPA). Chapter 1 in satellite rainfall applications for surface hydrology, doi:10.1007/978-90-481-2915-7, data provided by Asia-Pacific Data Research Center of the University of Hawaii at Manoa, accessed on 30 March 2018 http://apdrc.soest.hawaii.edu/dods/public_data/satellite_product/TRMM/TRMM_PR/3B43_monthly

Kida, S., & Richards, K. J. (2009). Seasonal sea surface temperature variability in the Indonesian seas. *Journal of Geophysical Research*, *114*(C6), C06016. https://doi.org/10.1029/2008JC005150

Kida, S., & Wijffels, S. (2012). The impact of the Indonesian Throughflow and tidal mixing on the summertime sea surface temperature in the western Indonesian Seas. *Journal of Geophysical Research*, *117*(C9). https://doi.org/10.1029/2012JC008162

Koch-Larrouy, A., Madec, G., Blanke, B., & Molcard, R. (2008). Water mass transformation along the Indonesian throughflow in an OGCM. *Ocean Dynamics*, *58*(3-4), 289–309. https://doi.org/10.1007/s10236-008-0155-4

Llovel, W., & Lee, T. (2015). Importance and origin of halosteric contribution to sea level change in the southeast Indian Ocean during 2005–2013. *Geophysical Research Letters*, *42*, 1148–1157. https://doi.org/10.1002/2014GL062611

Masumoto, Y., Sasaki, H., Kagimoto, T., Komori, N., Ishida, A., Sasai, Y., et al. (2004). A fifty-year eddy resolving simulation of the world ocean: Preliminary outcomes of OFES (OGCM for the Earth Simulator). *Journal of the Earth Simulator*, *1*, 35–56.

Meissner, T., & Wentz, F. J. (2016). Remote sensing systems SMAP ocean surface salinities, version 2.0 validated release. Remote Sensing Systems, Santa Rosa, CA, USA, data provided by Asia-Pacific Data Research Center of the University of Hawaii at Manoa, accessed on 29 March 2018, http://apdrc.soest.hawaii.edu/dods/public_data/PODAAC/smap_local

Meybeck, M., & Ragu, A. (1995). River discharges to the oceans: An assessment of suspended solids, major ions and nutrients. Environment Information and Assessment Report, UNEP.

Miyama, T., Awaji, T., Akitomo, K., & Imasato, N. (1996). A Lagrangian approach to the seasonal variation of salinity in the mixed layer of the Indonesian Seas. *Journal of Geophysical Research*, *101*(C5), 12,265–12,285. https://doi.org/10.1029/96JC00390

Nagai, T., & Hibiya, T. (2015). Internal tides and associated vertical mixing in the Indonesian Archipelago. *Journal of Geophysical Research: Oceans*, *120*, 3373–3390. https://doi.org/10.1002/2014JC010592

Neale, R., & Slingo, J. (2003). The Maritime Continent and its role in the global climate: A GCM study. *Journal of Climate*, *16*(5), 834–848. https://doi.org/10.1175/1520-0442(2003)016<0834:TMCAIR>2.0.CO;2

Paris, C. B., Helgers, J., Van Sebille, E., & Srinivasan, A. (2013). Connectivity Modeling System (CMS): A probabilistic modeling tool for the multiscale tracking of biotic and abiotic variability in the ocean. *Environmental Modelling & Software*, *42*, 47–54. https://doi.org/10.1016/j.envsoft.2012.12.006

Phillips, H. E., Wijffels, S. E., & Feng, M. (2005). Interannual variability in the freshwater content of the Indonesian-Australian Basin. *Geophysical Research Letters*, *32*, L03603. https://doi.org/10.1029/2004GL021755

Potemra, J. T., Hacker, P. W., Melnichenko, O., & Maximenko, N. (2016). Satellite estimate of freshwater exchange between the Indonesian Seas and the Indian Ocean via the Sunda Strait. *Journal of Geophysical Research: Oceans*, *121*, 5098–5111. https://doi.org/10.1002/2015JC011618

Sasaki, H., Kida, S., Furue, R., Nonaka, M., & Masumoto, Y. (2018). An increase of the Indonesian Throughflow by internal tidal mixing in a high-resolution quasi-global ocean simulation. *Geophysical Research Letters*, *45*, 8416–8424. https://doi.org/10.1029/2018GL078040

Sasaki, H., Nonaka, M., Masumoto, Y., Sasai, Y., Uehara, H., & Sakuma, H. (2008). An eddy-resolving hindcast simulation of the quasi-global ocean from 1950 to 2003 on the Earth Simulator. In K. Hamilton & W. Ohfuchi (Eds.), *High resolution numerical modelling of the atmosphere and ocean* (pp. 157–185). New York, NY: Springer. https://doi.org/10.1007/978-0-387-49791-4_10

Sprintall, J., Wijffels, S. E., Molcard, R., & Jaya, I. (2009). Direct estimates of the Indonesian Throughflow entering the Indian Ocean: 2004–2006. *Journal of Geophysical Research*, *114*(C7), C07001. https://doi.org/10.1029/2008JC005257

Susanto, R. D., Wei, Z., Adi, T. R., Zheng, Q., Fang, G., Fan, B., et al. (2016). Oceanography surrounding Krakatau Volcano in the Sunda Strait, Indonesia. *Oceanography*, *29*(2), 264–272. https://doi.org/10.5670/oceanog.2016.31

van Beek, E., Bons, K., & Brinkman, J. (2013). Joint Cooperation Program Activity Report January 2011–March 2013, Document B1.1, Final report Einlanden-Digul-Bikuma basin IWRM case study, https://publicwiki.deltares.nl/display/JCP/Final+Reports

Wijffels, S. E., Beggs, H., Griffin, C., Middleton, J. F., Cahill, M., King, E., et al. (2018). A fine spatial-scale sea surface temperature atlas of the Australian regional seas (SSTAARS): Seasonal variability and trends around Australasia and New Zealand revisited. *Journal of Marine Systems*, *187*, 156–196. https://doi.org/10.1016/j.jmarsys.2018.07.005

Wyrtki, K. (1961). Physical oceanography of the Southeast Asian waters. University of California, NAGA Rept., No. 2, 195 pp.

Yamanaka, M. D., Ogino, S. Y., Wu, P. M., Jun-Ichi, H., Mori, S., Matsumoto, J., & Syamsudin, F. (2018). Maritime continent coastlines controlling Earth's climate. *Progress in Earth and Planetary Science*, *5*(1), 21. https://doi.org/10.1186/s40645-018-0174-9

Zhang, N., Feng, M., Du, Y., Lan, J., & Wijffels, S. E. (2016). Seasonal and interannual variations of mixed layer salinity in the southeast tropical Indian Ocean. *Journal of Geophysical Research: Oceans*, *121*, 4716–4731. https://doi.org/10.1002/2016JC011854